J Mater Sci (2011) 46:117–122
DOI 10.1007/s10853-010-4858-9

Effect of ion exchange on *R*-curve behavior of a dental porcelain

Paulo Francisco Cesar · Vinicius Rosa · Marcelo Mendes Pinto · Humberto Naoyuki Yoshimura · Luoyu Roy Xu

Received: 26 February 2010 / Accepted: 20 August 2010 / Published online: 14 September 2010

Abstract The objective of this study was to evaluate the effect of the ion exchange treatment on the *R*-curve behavior of a leucite-reinforced dental porcelain, testing the hypothesis that the ion exchange is able to improve the *R*-curve behavior of the porcelain studied. Porcelain disks were sintered, finely polished, and submitted to an ion exchange treatment with a KNO_3 paste. The *R*-curve behavior was assessed by fracturing the specimens in a biaxial flexure design after making Vickers indentations in the center of the polished surface with loads of 1.8, 3.1, 4.9, 9.8, 31.4, and 49.0 N. The results showed that the ion exchange process resulted in significant improvements in terms of fracture toughness and flexural strength as compared to the untreated material. Nevertheless, the rising *R*-curve behavior previously observed in the control group disappeared after the ion exchange treatment, i.e., fracture toughness did not increase with the increase in crack size for the treated group.

P. F. Cesar · V. Rosa
Department of Dental Materials, School of Dentistry, University of São Paulo, São Paulo, Brazil

M. M. Pinto
Universidade Nove de Julho (UNINOVE), São Paulo, Brazil

H. N. Yoshimura
Center for Engineering, Modeling and Applied Social Science, Federal University of ABC, Santo André, Brazil

L. R. Xu
Department of Civil and Environmental Engineering, Vanderbilt University, Nashville, TN, USA

P. F. Cesar (✉)
Departamento de Materiais Dentários, Faculdade de Odontologia, Universidade de São Paulo, Av. Prof. Lineu Prestes, 2227–Cidade Universitária "Armando Salles de Oliveira", São Paulo, SP 05508-900, Brazil
e-mail: paulofc@usp.br

Introduction

Ceramic materials present a rising resistance curve (*R*-curve) behavior when the fracture toughness increases with crack extension. Such a rising fracture resistance with crack extension has been observed in a number of biological and synthetic materials of interest for dentistry, such as cortical bone [1], dentin [2], enamel [3], dental ceramics [4], and dental resin composites [5, 6].

R-curves are a consequence of energy-consuming effects such as toughening mechanisms which can be either due to the crack front or crack wake effects [7]. Microcracking, microvoid formation, and crack branching are considered crack front effects (or intrinsic mechanisms), as they take place ahead of the crack tip, where a disturbed material zone (process zone) extends with increasing load. If this damaged zone ahead of the main crack is stable from the onset of crack extension, no rising *R*-curve is expected. However, if this zone increases with the increasing crack extension, a rising crack growth resistance curve exists [8, 9]. Such intrinsic mechanisms are an inherent property of the material and are considered the principal means by which ductile materials like metals obtain their toughness. Due to the lack of plastic transformation in ceramics, intrinsic toughening mechanisms are not so frequently observed [7]. Another crack front effect is the in situ phase transformation as observed in transformation-toughened zirconia which undergoes a stress-induced martensitic transformation from the tetragonal to the monoclinic phase in front of a crack. In this case, during crack growth, the *R*-curve increases till a steady state transformation zone is developed [10].

Crack wake effects (extrinsic mechanisms) are caused by the crack border interaction in the wake of an advancing crack [11]. As opposed to intrinsic mechanisms that affect primarily the initiation of the crack, extrinsic toughening mechanisms become more active as the crack propagates, and that is why they are also known as "mechanisms of crack growth toughening" [7]. Crack wake effects may be caused by frictional sliding bridges and mechanically interlocking bridges caused by crack deflection due to interparticle/intercluster crack growth, which act to arrest the crack tip opening [12–14]. Such toughening mechanisms have been observed in fiber-reinforced composites [15] and coarse-grained polycrystalline ceramics [16]. For alumina ceramics with grain sizes around 20 μm, the grain bridging occurs as a result of intergranular fracture and an increase in fracture toughness from 2 to 6 MPa $m^{1/2}$ has been observed with the increase in crack size from 1 to 5 mm [17]. It has also been demonstrated for dental porcelains that crack deflection around leucite particles results in rough crack surfaces which will cause mechanical grip between the two surfaces of the crack wake, shielding the crack tip and increasing fracture toughness as consequence of the increase in crack size [18]. In situ phase transformation like the one observed in partially stabilized zirconia is also considered as an extrinsic toughening mechanism by some authors, since the dilated zone may also surround the crack wake, therefore progressively reducing the near-tip stress intensity [7].

The above mentioned toughening mechanisms will ultimately shield the crack from some of the applied load, reducing the intensification of stresses around the crack tip. Due to the increase of fracture resistance with crack extension, additional energy is necessary for a crack to propagate until failure of the component [19]. In other words, these toughening mechanisms are responsible for lowering the near-tip stress intensity, K_{tip}, in relation to the applied stress intensity, K_{app}, as follows:

$$K_{tip} = K_{app} - K_{br} \quad (1)$$

where K_{br} is the bridging stress intensity, which is a function of the crack extension [5]. Therefore, the *R*-curve behavior is more dominant for larger cracks than smaller cracks, because the friction at the border of the crack tip increases with the increase in the crack size [4].

Several studies that assessed the correlation between fracture toughness and the crack size showed that during initial crack growth, the fracture toughness increases significantly and after a certain crack length, it stabilizes forming a plateau [5, 19]. The observation of a steady state toughness following the initial toughness increase with increasing crack size indicates that the bridges are forming and breaking at approximately equivalent rates in the crack wake [5].

The *R*-curve behavior in ceramic materials may be experimentally characterized by obtaining plots of fracture resistance, K_R, as a function of the crack length. These curves may be obtained by using standard fracture mechanics compact tension specimens in which a micronotch is produced. The specimen is then loaded and unloaded intermittently in order to create and extend a sharp pre-crack. Measurement of the different pre-cracks sizes is then performed and applied to the standard fracture mechanics based solution for the compact tension specimen [5]. Another widely used method for evaluating the *R*-curve in ceramic materials is the indentation flexural strength test [20], in which bar or disk specimens are indented with a Vickers diamond point before being fast fractured in a flexural strength test. Different magnitudes of indentation loads are used in order to create different crack sizes which are correlated with the bending strength. Furthermore, crack growth relations for *R*-curve characterization may be achieved by measurements of cracks extending from natural flaws, or by means of indirect methods that allow for determination of the relations between K_R and the crack extension from the measurements of strength or lifetime [9]. These different methodologies often give dissimilar results; therefore, the test method should be taken into consideration when comparing *R*-curves from different works. The indentation technique which was used in the present study has the advantage of measuring short cracks, which are of the order of the sizes of natural cracks [9]. Other advantages of this technique may be mentioned like the fact that the methodology is very straightforward and the small amount of material required to carry out the tests.

The exchange of small host alkali ions (Na^+) for larger alkali ions (K^+) from an external source such as a molten salt bath of potassium nitrate (KNO_3) in a porcelain's glassy matrix below its strain temperature is known as ion exchange process. The large ions remain essentially "stuffed" in the glass network interstitial sites originally occupied by the small ions leading to a two-dimensional state of compressive stress, since the bulk material restrains the expansion of the surface structure which acquires a different chemical composition [21]. The need of long soaking times (i.e. up to 24 h for commercial soda-lime silica glass) has rendered to this technique a limitation for its application [22]. The introduction of the paste technique, in which a KNO_3 paste is used for shorter heat-treatment times (from 15 to 30 min) to induce the ion exchange was proved to be effective not only by enhancing dental porcelain's flexural strength and fracture toughness [21] but also by decreasing its susceptibility to slow crack growth [23]. However, the effect of this chemical treatment on the *R*-curve properties of dental porcelains has not been determined yet. Therefore, the objective of this study is to

evaluate the effect of ion exchange on the *R*-curve behavior of a leucite-reinforced dental porcelain, testing the hypothesis that the ion exchange is able to improve the *R*-curve behavior of the porcelain studied.

Materials and methods

One hundred and four specimens were fabricated by one single operator by mixing 1 g of a leucite-reinforced porcelain powder (Ultropaline Super Transparent, Jen Dental, Kiev, Ukrain, batch: 1094) with 0.4 mL of deionized water in order to form a slurry that was poured into a metal mold to obtain disk-shaped specimens (15 mm in diameter and 3 mm in thickness). Specimens were vacuum-fired in a porcelain furnace (Keramat I, Knebel, Porto Alegre, Brazil) according to manufacturer's instructions. After sintering, the specimens measuring 12.5 mm in diameter and 2.4 mm in thickness were machined in a surface-grinding device (MSG-600, Mitutoyo, São Paulo, Brazil) following the guidelines in ASTM C 1161 [24] to obtain parallel surfaces and reduce thickness to 1.3 mm. Then, one of their surfaces was mirror-polished using a polishing machine (Ecomet 2, Buehler, Lake Bluff, USA) with diamond suspensions up to 1 μm to obtain the final thickness of 1.0 (±0.1) mm.

The ion exchange strengthening treatment by paste method was performed in 52 specimens. The paste was prepared by mixing 10 g of reagent grade KNO_3 salt (Merck, Damstadt, Germany) with 4 mL of deionized water; 0.4 g of this paste was deposited on the polished surface of each specimen and then they were heat treated in an electric oven (FP-32, Yamato, Tokyo, Japan) at a heating rate of 5 °C/min, an intermediary step at 150 °C for 20 min for paste drying, and a holding time of 15 min at 470 °C to promote the ion exchange process. The effectiveness of ion treatment was assessed by the chemical composition of the material before and after ion exchange using chemical microanalysis by energy dispersive spectroscopy (EDS; Noran Instruments, Middletown, USA) coupled to a scanning electron microscope (SEM; Jeol – JSM 6300, Peabody, MA, USA). The relative peak intensities of the sodium and potassium before and after ion exchange treatment were calculated as a fraction of the silicon peak intensity [25]. The Na_2O and K_2O contents were determined using the results of chemical analysis (XRF 1500, Shimadzu, Tokio, Japan) of the starting powder and the relative peak intensities of sodium and potassium elements.

For the assessment of the *R*-curve behavior, a Vickers indentation was impressed (dwell time of 20 s) in the center of the polished surface of seven specimens of each group with the following indentation loads (N): 1.8; 3.1; 4.9; 9.8; 31.4; and 49.0. Then, the specimens were stored in air (~60% relative humidity and 22 °C) for 24 h in order to stabilize the slow crack growth [26] and tested for the measurement of biaxial flexure strength (σ_f) using the piston-on-three-balls method (ASTM F394-78 [27]) in a universal testing machine (Syntech 5G, MTS, São Paulo, Brazil) at a constant stress rate of 10 MPa/s with the specimen immersed in artificial saliva [100 mL of KH_2PO_4 (2.5 mM); 100 mL of Na_2HPO_4 (2.4 mM); 100 mL of $KHCO_3$ (1.5 mM); 100 mL of NaCl (1.0 mM); 100 mL of $MgCl_2$ (0.15 mM); 100 mL of $CaCl_2$ (1.5 mM); and 6 mL of citric acid (0.002 mM)] [28] heated and maintained constant at 37 °C. The biaxial flexural strength (σ_f) was calculated according to [27]:

$$\sigma_f = -0.2387P(X - Y)/d^2 \quad (2)$$

where σ_f is the maximum tensile stress, P is the load at fracture, and d is the specimen thickness at fracture origin. X and Y were determined as follows:

$$X = (1 + \nu)\ln(B/C)^2 + [(1-\nu)/2)](B/C)^2 \quad (3)$$

$$Y = (1 + \nu)[1 + \ln(A/C)^2] + (1-\nu)(A/C)^2 \quad (4)$$

where ν is the Poisson's ratio, A is the radius of the support circle, B is the radius of the tip of the piston, and C is the radius of the specimen. The value of υ (0.22) was determined by the ultrasonic pulse-echo method [29] using a 200 MHz ultrasonic pulser-receiver (Panametrics, USA, 5900 PR), 20 MHz longitudinal and shear transducers with a delay material, and a coupling paste (Panametrics) applied between the sample and transducer [30].

The estimation of K_{Ic} as a function of the crack extension was made according to the relations presented in a previous study [31]:

$$K_{Ic} = k(\Delta a)^q \quad (5)$$

where k and q are constants and Δa is the crack extension.

In order to determine k and q, the results obtained for flexural strength were plotted as a function of the indentation load. The regression curve obtained from these data is given by [31]:

$$\sigma_f = \alpha \cdot P^{-\beta} \quad (6)$$

where σ_f is the flexural strength, α is the intercept with the abscissa, $-\beta$ is the slope of the fit line (material parameters), and P is the indentation load. Once the β value is determined, it is possible to calculate the exponent q using Eq. 7. Whenever β is equal to or higher than 1/3, the rising *R*-curve behavior is not observed [31].

$$q = \frac{1 - 3\beta}{2 + 2\beta} \quad (7)$$

The constant k is then obtained using Eq. 8, where $Y = 1.24$ for semicircular cracks [32] and γ is calculated according to Eq. 9 where a is the crack size [31].

$$k = \left[\frac{Y\alpha}{(\beta\gamma)^{\beta}}\right] \cdot (1+\beta)^{(1+\beta)} \quad (8)$$

$$\gamma = \frac{P}{a^{\left(\frac{2}{1+\beta}\right)}} \quad (9)$$

Results

The variations of sodium and potassium concentration in the porcelain's glassy matrix before and after the ion exchange treatment are shown in Table 1. It is possible to note that, as expected, there was a decrease in the sodium and an increase in the potassium content, confirming the occurrence of the ion exchange process. The sodium content decreased by a factor of 4, and the potassium content showed a twofold increase.

Figure 1 shows the flexural strength data as function of the indentation load applied for both experimental groups. It is possible to note that the flexural strength decreases as the applied load increases, since larger defects (indentations) result in lower strength. However, it is important to note that the drop in flexural strength was much more pronounced for the ion-exchanged group compared to the control, what is evidenced by the significantly higher slope of the fitted curve of the first. This difference in the slopes of the curves shows that the flaw size affected more the strength of the ion-exchanged specimens then that of the untreated ones.

In Fig. 1, the dashed line on the upper right hand of the plot has a slope of $-1/3$ ($\beta = 0.33$) and represents a material with flat *R*-curve, that is, fracture toughness is independent on the crack extension, as predicted by Eqs. 5 and 7. Therefore, whenever the value of β for one material is equal to or higher than the value of 0.33, it means that the material has a flat *R*-curve, and materials with value of β lower than that (lower slope) present a rising *R*-curve.

The values of α, β, and q, obtained from Eqs. 5 through 8, are shown in Table 2 for both experimental groups. Based on the β values, it is possible to infer that the control group did showed a rising *R*-curve behavior ($\beta = 0.115$), however the treated group had flat *R*-curve since its β value (0.343) was close to the threshold of 0.33.

The presence of the *R*-curve behavior in the control group is evidenced by Fig. 2, in which the fracture toughness was plotted as a function of the size of the indentation crack ($2c$). In this plot, it is possible to clearly note that for the control group there was an increase in fracture toughness from 0.39 to 0.56 MPa $m^{1/2}$ when the crack size increased from 30 to 480 μm. Conversely, a significant drop in fracture toughness from 1.3 to 0.8 MPa $m^{1/2}$ can be observed for the ion-exchanged group after the crack size increased from 20 to 250 μm. This means that no *R*-curve behavior is present in the treated group. Figure 3 shows the variation in flexural strength as a

Table 1 Na_2O and K_2O contents (wt%) in the vitreous matrix of the porcelain tested before and after the ion exchange treatment

Group	Na_2O	K_2O
Control	4.3	11.3
Ion exchange	1.2	20.6

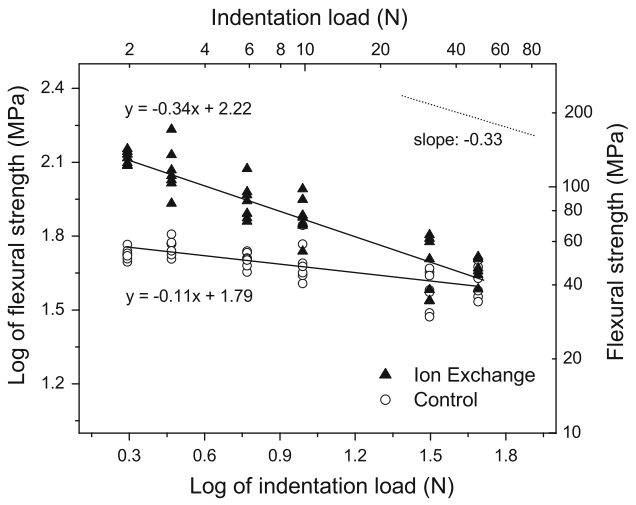

Fig. 1 Plot of flexural strength as a function of indentation load for both control and ion-exchanged experimental groups. *Dashed line* represents a material with flat *R*-curve

Table 2 Values of α, β, and q for both groups

Group	α	β	q
Control	61.5	0.115	0.29
Ion exchange	164.2	0.343	−0.01

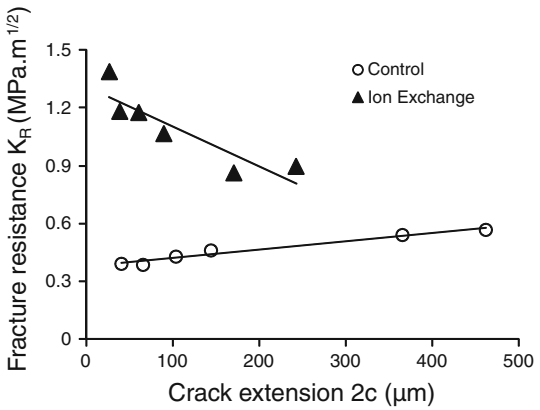

Fig. 2 Plot of fracture resistance calculated as a function of crack extension (2c)

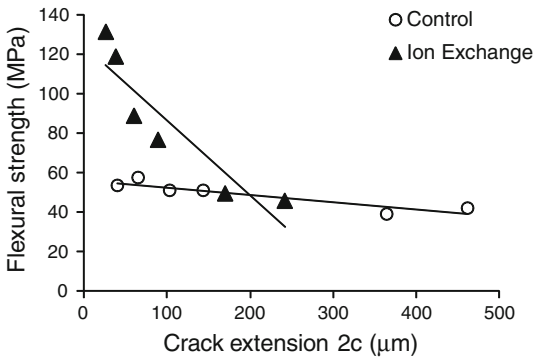

Fig. 3 Plot of flexural strength as a function of crack extension (2c)

function of the radial crack size. It is possible to note a much steeper decrease in strength as function of crack size for the ion-exchanged group compared to the control.

Discussion

The presence of a rising *R*-curve in the control group was somewhat expected since previous studies have demonstrated that leucite-reinforced dental ceramics exhibit an increase in fracture toughness with the increase in flaw size [18, 31, 33]. The *R*-curve behavior of the porcelain material is evident in the results shown in both Figs. 1 and 2. In Fig. 1, it is possible to note that for the control group the decrease in strength with the increase in the indentation load is not very pronounced, i.e., the slope of the fitted curve is not very high, indicating that the indentation load had little influence on the strength values, which is the type of behavior expected in materials with rising *R*-curve. In Fig. 2, the rising *R*-curve of the control group is also evident because the fracture toughness values gradually increased with the increase in crack size.

The *R*-curve behavior observed in the control group is a consequence of the crack wake effect caused by crack border interactions in the wake of the indentation radial crack [11]. A previous work has shown for leucite-based porcelains that the main toughening mechanism occurring during crack propagation is crack deflection around leucite particles and clusters, which results in a relatively rough fracture surface. The friction between these two rough surfaces will cause mechanical grip and act to close the crack [12], consequently shielding the crack tip from some of the applied load [13]. Such toughening mechanism will ultimately lower the near-tip stress intensity, K_{tip}, in relation to the applied stress intensity, K_{app}, as shown in Eq. 1. Therefore, the increase in crack size results in an increase in crack border interactions and consequently the measured fracture toughness also increases as seen in Fig. 2 (control group).

The results of flexural strength and fracture toughness of the present study indicated that the ion exchange treatment was capable of improving these properties for the porcelain studied. However, such improvements were much more noticeable when these properties were measured using small cracks. In Fig. 3, it is possible to note that for the small crack range (from ~30 up to ~100 μm) the increase in flexural strength after the ion exchange treatment was as high as 100%. With regard to fracture toughness (Fig. 2), significant increases in the mean values were observed regardless of the crack size, however for the smaller crack sizes (from 30 to 100 μm), there were significant increases in K_{Ic} up to 250%. The observed increase in mechanical properties is a result of the well known effects of the ion exchange process, in which a compressive layer is created on the material's surface due to the replacement of small sodium ions for larger potassium ions in the porcelain's glassy matrix. Because of this surface modification, cracks in the porcelain will only propagate when the stresses generated during loading overcome the residual stresses induced by the compressive layer at the surface. Previous studies have already shown that these compressive stresses result in a significant increase in both flexural strength and fracture toughness of leucite-based porcelains [34, 35].

Apart from the evidences of increased mechanical properties after the ion exchange process, it is important to note that for larger crack sizes, that is, 2c larger than ~150 μm, no significant improvements were observed in the flexural strength values (Fig. 3). It is probable that for larger crack lengths in the range of ~200 μm the ion exchange process was not so effective in generating compressive stresses throughout the whole crack structure. Therefore, while the smaller defects, generated by lower loads, were totally surrounded by the compression stresses, it is likely that larger flaws were only partially surrounded, what may have hindered further improvements in the flexural strength of the porcelain. The ion exchange process results in a residual compressive stress profile with the maximum value at the surface which decreases with the increase in depth from the surface [23]. As a consequence, it seems that this residual stress profile causes a negative, or a decreasing *R*-curve component, which counteracts and annuls the positive, or rising *R*-curve component caused by the microstructure (leucite particles). This statement is supported by the results of a proposed two-step ion exchange method, in which a short second ion exchange process in a 30% Na_2O–70% K_2O bath is carried out for partial removal of the K^+ ions introduced in the first extended treatment [36]. The second step causes the displacement of the maximum compressive stress to a given distance from the surface, causing a rising *R*-curve up to this depth [36]. Residual surface stress profiles of different

ion exchange processes can be found elsewhere for reference [23].

The results of the present study showed that the introduction of residual compressive stresses had a negative effect on the *R*-curve behavior of the porcelain studied, since before the ion exchange treatment the material presented a clear rising *R*-curve, and after the treatment this behavior was not present anymore, as demonstrated in Fig. 2. Therefore, the hypothesis that the ion exchange process would improve the *R*-curve behavior of the porcelain had to be rejected. One possible explanation for the change in the material's behavior in terms of *R*-curve is that there is a significant difference in the range of crack sizes when the control and treated group are compared. By observing Fig. 2, it is noted that for the control group, crack sizes varied from $\sim$30 up to $\sim$500 μm, and the most significant increases in fracture toughness occurred after the indentation crack reached $\sim$100 μm. On the other hand, for the ion-exchanged group, the presence of residual compression stresses on the surface of the material hindered the propagation of the indentation crack, resulting in smaller crack sizes varying from $\sim$30 up to 250 μm. Therefore, this smaller crack range in the ion-exchanged group may have in part accounted for the absence of an rising *R*-curve in this group since it has been demonstrated that the *R*-curve behavior is more evident for larger than for smaller cracks, because the friction at the border of the crack tip increases with the increase in crack size [4]. Another possible explanation for the vanishing of the rising *R*-curve behavior after the ion exchange treatment is the fact that the presence of residual compressive stresses around the radial cracks in the range depicted in Fig. 2 somehow superimposes the frictional grip effect observed between the crack walls and consequently the fracture toughness did not increase with the increase in crack size.

Conclusion

In conclusion, the results of this study showed that when an a dental porcelain is toughened by means of an ion exchange process, the rising *R*-curve behavior previously observed in the control group disappears, as the fracture toughness did not increase with the increase in crack size. However, it is important to note that apart from the absence of a rising *R*-curve on the ion-exchanged material, the ion exchange process resulted in significant improvements in terms of fracture toughness and flexural strength as compared to the untreated material, which should be taken into consideration as a positive achievement for the application of such materials.

Acknowledgements The authors acknowledge the Brazilian agencies FAPESP, CNPq and CAPES for the financial support of the present research.

References

1. Nalla RK, Kruzic JJ, Ritchie RO (2004) Bone 34:790
2. Nazari A, Bajaj D, Zhang D, Romberg E, Arola D (2009) J Mech Behav Biomed Mater 2:550
3. Bajaj D, Arola DD (2009) Biomaterials 30:4037
4. Fischer H, Rentzsch W, Marx R (2002) J Dent Res 81:547
5. Shah MB, Ferracane JL, Kruzic JJ (2009) Dent Mater 25:760
6. Shah MB, Ferracane JL, Kruzic JJ (2009) J Mech Behav Biomed Mater 2:502
7. Launey ME, Ritchie RO (2009) Adv Mater 21:2103
8. Nairn JA (2009) Int J Fract 155:167
9. Munz D (2007) J Am Ceram Soc 90:1
10. Swain MV (1985) Acta Metall 33:2083
11. Swanson PL, Fairbanks CJ, Lawn BR, Mai YW, Hockey BJ (1987) J Am Ceram Soc 70:279
12. Fett T, Munz D (1993) J Mater Sci 28:742. doi:10.1007/BF01151251
13. Steinbrech RW, Reichl A, Schaarwachter W (1990) J Am Ceram Soc 73:2009
14. Rodel J (1992) J Eur Ceram Soc 10:143
15. Medeiros IS, Luz LA, Yoshimura HN, Cesar PF, Hernandes AC (2009) J Mech Behav Biomed Mater 2:471
16. Kruzic JJ, Satet RL, Hoffmann MJ, Cannon RM, Ritchie RO (2008) J Am Ceram Soc 91:1986
17. Chantikul P, Bennison SJ, Lawn BR (1990) J Am Ceram Soc 73:2419
18. Yoshimura HN, Cesar PF, Miranda WG, Okada CY, Goldenstein H, Gonzaga CC (2005) J Am Ceram Soc 88:1680
19. Rodriguez-Suarez T, Lopez-Esteban S, Pecharroman C et al (2009) Acta Mater 57:2121
20. Krause RF (1988) J Am Ceram Soc 71:338
21. Cesar PF, Gonzaga CC, Miranda WG Jr, Yoshimura HN (2007) J Biomed Mater Res B 83:538
22. Sinton CW, Lacourse WC, O'Connell MJ (1999) Mater Res Bull 34:2351
23. Rosa V, Yoshimura HN, Pinto MM, Fredericci C, Cesar PF (2009) Dent Mater 25:736
24. ASTM (2002) C 1161 Flexural strength of advanced ceramics at ambient temperature. American Society for Testing Materials
25. Lange FF, Hirlinger MM (1985) J Mater Sci Lett 4:1437
26. Cesar PF, Soki FN, Yoshimura HN, Gonzaga CC, Styopkin V (2008) Dent Mater 24:1114
27. ASTM Designation (Reapproved 1991) American Society for Testing Materials; F394-78, Philadelphia, PA
28. Cate JMT, Duijisters PPE (1982) Caries Res 16:201
29. JIS (1986) Testing methods for elastic modulus of high performance ceramics. JIS R 1602: 216
30. Yoshimura HN, Molisani AL, Narita NE, Cesar PF, Goldenstein H (2007) Mater Res 10:127
31. Fischer H, Rentzsch W, Marx R (2002) J Dent Res 8:547
32. Quinn GD (2007) Fractography of ceramics and glasses. U.S. Government Printing Office, Washington
33. Pinto MM, Cesar PF, Rosa V, Yoshimura HN (2008) Dent Mater 24:814
34. Fischer H, Marx R (2003) J Biomed Mater Res A 66:885
35. Seghi RR, Crispin BC, Mito W (1990) Int J Prosthodont 3:130
36. Green DJ, Tandon R, Sglavo VM (1999) Science 283:1295